Available online at www.sciencedirect.com
ScienceDirect
Nuclear Instruments and Methods in Physics Research A 581 (2007) 461–464
NUCLEAR INSTRUMENTS & METHODS IN PHYSICS RESEARCH Section A
www.elsevier.com/locate/nima

Single photon timing resolution and detection efficiency of the IRST silicon photo-multipliers

G. Collazuol[a,b,*], G. Ambrosi[f], M. Boscardin[d], F. Corsi[h], G.F. Dalla Betta[g], A. Del Guerra[b,c], N. Dinu[g], M. Galimberti[e], D. Giulietti[b,c,e], L.A. Gizzi[b,e], L. Labate[b,e], G. Llosa[b,c], S. Marcatili[b,c], F. Morsani[b], C. Piemonte[d], A. Pozza[d], L. Zaccarelli[b], N. Zorzi[d]

[a]*Scuola Normale Superiore, 56127 Pisa, Italy*
[b]*INFN Sezione di Pisa, 56127 Pisa, Italy*
[c]*Dipartimento di Fisica, Università di Pisa, 56127 Pisa, Italy*
[d]*Fondazione Bruno Kessler - IRST, Divisione Microsistemi, 38050 Trento, Italy*
[e]*Intense Laser Irradiation Laboratory, IPCF-CNR, 56127 Pisa, Italy*
[f]*INFN Sezione di Perugia, 06123 Perugia, Italy*
[g]*INFN Sezione di Padova, Gruppo Collegato di Trento, 38050 Trento, Italy*
[h]*DEE—Politecnico di Bari and INFN Sezione di Bari, 70125 Bari, Italy*

Available online 7 August 2007

Abstract

Silicon photo-multipliers (SiPM) consist in matrices of tiny, passive quenched avalanche photo-diode cells connected in parallel via integrated resistors and operated in Geiger mode. Novel types of SiPM are being developed at FBK-IRST (Trento, Italy). Despite their classical shallow junction n-on-p structure the devices are unique in their enhanced photo-detection efficiency (PDE) for short-wavelengths and in their low level of dark rate and excess noise factor. After a summary of the extensive SiPM characterization we will focus on the study of PDE and the single photon timing resolution.
© 2007 Elsevier B.V. All rights reserved.

PACS: 29.40.Wk; 85.60.Gz; 85.60.Bt; 95.55.−n; 42.65.Re

Keywords: Silicon photomultiplier; Opto-semiconductor; Photon detection efficiency; High resolution timing; Single photon

1. Introduction

High efficiency in detecting low optical photon fluxes with unprecedented amplitude resolution, extreme single photon timing resolution, low voltage operation and insensitivity to magnetic fields make silicon photo-multipliers suitable for many applications. Novel types of SiPM's are being developed at IRST since 2005 within the framework of the DASIPM collaboration between the two Italian institutes of INFN and Fondazione Bruno Kessler—IRST. DASIPM is focusing on the development and applications of SiPM's in Medical, Space and High Energy Physics.

A typical IRST prototype [1] is a matrix of 25×25 photo-diode cells covering a surface of $1 \times 1\,\mathrm{mm}^2$. The structure of each diode consists of an asymmetric very shallow (100 nm) junction n^+-p implanted in a thin ($\sim$4 μm) lowly doped p-type epitaxial layer (epi-layer). The structure is grown on a low-resistivity p^+-type substrate ($\sim$500 μm). The main active volume to photo-generate carriers is the fully depleted epi-layer, with a typical effective area of $30 \times 30\,\mu\mathrm{m}$.

When diodes are biased at few volts above breakdown (V_{BD}) and non-conducting, the electric field in the junction region is so high that any single carrier, generated either thermally or by photons, and drifted in that region, may

*Corresponding author. Scuola Normale Superiore, 56127 Pisa, Italy. Tel.: +39 050 2214 222.
E-mail address: gianmaria.collazuol@pi.infn.it (G. Collazuol).

0168-9002/$ - see front matter © 2007 Elsevier B.V. All rights reserved.
doi:10.1016/j.nima.2007.08.027

trigger a self-sustaining avalanche. While a swift current (sub-nanosecond rise-time) grows to a macroscopic level (μA range) it flows through a series resistor R_Q developing a voltage drop which quenches the avalanche by reducing the bias voltage. Thereafter the original over-voltage is exponentially recovered within a time scale of ~50 ns.

Unique feature of IRST devices is the improved detection efficiency for short wavelengths. The number of collected photo-generated carriers is enhanced by means of: (i) an optimized anti-reflective coating (ARC), (ii) a very shallow junction, (iii) a minimized recombination probability in the n^+ region and at the Oxide-Si interface and (iv) a thin high-field (multiplication) region. More details can be found in Ref. [1].

Characterization [2,3] under standard working conditions, i.e. over-voltage range $\Delta V \sim 1-5$ V and room temperature are summarized as follows.

(i) Gain ($\sim 10^6$) is linear with ΔV, which demonstrates the effectiveness of the avalanche quenching mechanism and allows for a very good resolution (few %) on the collected charge due to the high cell-to-cell uniformity of the response. The relative gain variation with bias voltage and temperature are, respectively, $\delta G/G/\delta V \sim 1\%/20\,\text{mV}$ and $\delta G/G/\delta T \sim 4\%/^\circ\text{C}$ at $G \sim 10^6$.
(ii) *I-V* curve at dark shows good reproducibility and parameters uniformity both within a wafer and from wafer to wafer. The dark rate at single photo-electron threshold is at the level of 1 MHz. Relevant improvement is expected there.
(iii) Under standard conditions after-pulse and cross-talk probabilities are limited to few %, growing quadratically with ΔV.

2. Photo-detection efficiency

Photo-detection efficiency (PDE) as a function of wavelength (λ) and over-voltage (ΔV) was measured at IRST [3]. The setup included a calibrated white light source and a monochromator (wavelength range 380−800 nm). The photon flux was kept below 15kHz per cell in order to avoid saturation effects in the SiPM.

The number of photo-electrons was measured in two ways. The first method consists in measuring the DC current under illumination, subtracting the dark DC current and dividing by the gain. The second method does not require the measurement of the gain. It consists in counting the rate of pulses above a threshold ($\geqslant 1$ photo-electrons) and subtracting the dark count rate. The uncertainty on the measurements is at the level of 10% relative. Agreement between the two methods indicates that the effects of after-pulses and cross-talk are within the errors.

PDE for a device with fill factor of 20% is shown as a function of the wavelength (λ) in Fig. 1, whose shape can be explained as follows. PDE is a product of three factors: the quantum efficiency (QE) including the transmittance T_{in} through the entrance window, the probability P_{t} to trigger an avalanche and the fill factor (A_{e}). A_{e} is an upper limit for the PDE, being independent of ΔV and λ. QE depends on λ via both the transmittance T_{in} through the anti-reflective coating (ARC) and the probability for a photo-generated carrier to reach the high-field region (internal quantum efficiency). P_{t} depends [4] on the impact ionization rate, hence on ΔV, and on the position of the generated carrier: at short λ only holes from the n^+ region enter the junction and may trigger the avalanche, while at long λ only electrons drifting from the depletion region may do it.

PDE is found to be linear with ΔV up to few volts, as expected from the triggering probability models [4].

Concerning the dependence of PDE on λ, in order to disentangle the contributions from P_{t} and QE, the latter was directly measured on diodes extracted from the same wafers as the SiPM under investigation, and having the same anti-reflective coating and doping profiles but no quenching resistor. QE was measured in photo-voltaic regime (V_{bias} range ~0−5 V). The measurement is in agreement with TCAD simulations of internal quantum efficiency and with the expected transmittance [3]. Due to the technological choices at IRST, QE is quite high (>90%) for wavelengths ranging from 380 to 530 nm. The decrease of QE at small λ is caused by the poor transmittance of the ARC, while the slow QE reduction at long λ is due to the thickness of the epitaxial layer.

The ratio between the measured PDE and QE yields P_{t}, which is found to saturate at a maximum above $\lambda > 550$ nm and at a minimum below $\lambda < 400$ nm. The ratio between the maximum and minimum is about 2, consistently with the ratio between the impact ionization rate of electrons and holes.

3. Single photon timing resolution

The time resolution to single photons was studied by illuminating SiPM's with ultra-short laser pulses at fixed repetition rate and measuring the fluctuations of the difference in time between successive pulses.

Measurements were carried out at the IPCF-CNR laboratory (Pisa) where a mode-locked Ti:sapphire laser, pumped by a continuous-wave solid-state green laser, provides red light ($\lambda = 800$ nm) pulses ~60 fs wide at a repetition rate of ~80 MHz, with jitter below 100 fs. Data were collected also at $\lambda = 400$ nm by exploiting a second harmonic generation crystal. After being filtered to the proper low intensity, the beam entered a black box, for rejecting environment light and electromagnetic noise, and the spot (~2 cm in diameter) impinged on the SiPM. The electronics to readout the SiPM current through a series resistor consisted in an AC coupled voltage amplifier (gain ~ × 50) based on a low-noise and wide-band RF monolithic amplifier (gali-5, MiniCircuits) with low input impedance (50 Ω). The amplifier output was sampled at 20 GSamples/s by a LeCroy SDA 6020 digital oscilloscope with 6 GHz analog bandwidth (acknowledgments to E. Marcon, Lecroy).

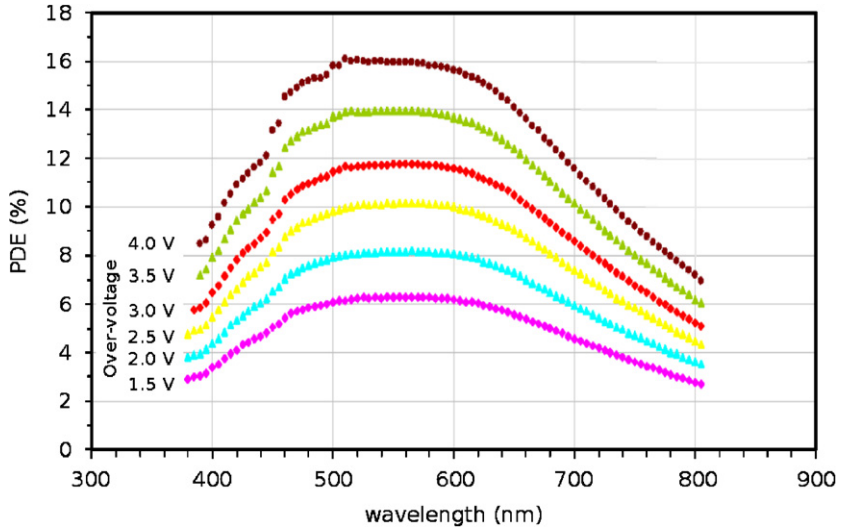

Fig. 1. Photo-detection efficiency as a function of wavelength at various over-voltages for a device with fill factor of $A_e = 20\%$.

Different sets of data were collected for each device at $\lambda = 800$ and 400 nm, by varying the over-voltage (ΔV) and the light intensity conditions, but always keeping the rate on the single SiPM cell in the range 15−30 kHz.

The analysis of each set of data consists first in selecting single photo-electron signals (s.p.e. peaks) by requiring proper signal shape, pulse height and width. Typical rise-time and FWHM width are ~1 and ~3 ns, respectively. Low instantaneous intensity and low noise are obtained by requiring absence of additional peaks and voltage fluctuations below 1 mV r.m.s., respectively, within an interval of ±50 ns around the selected s.p.e. peak.

To reconstruct the s.p.e. time with minimized effect from the electronic white noise a zero crossing filter [5] is applied as follows: first a "reference" s.p.e. signal $V_r(t - t_0)$ is built unaffected by the noise and depending on a reference time t_0. Then $V_r(t - t_0)$ is slid along the time axis, by varying the reference time t_0, until a best fit to the measured s.p.e. signal $V_a(t)$ is obtained. The condition of optimum timing is given by solving in t_0 the following eq. $\int(\partial V_r(t - t_0)/\partial t)V_a(t)\,dt = 0$. Finally, the fluctuations of the SIPM response time are studied by taking the difference between successive s.p.e. peaks modulo the measured laser period ($T = 12.367$ ns).

In almost every set of measurements it is found that the distribution of time differences for data at $\lambda = 400$ nm fits (with good χ^2) to a gaussian plus a constant term, the latter being consistent with the contribution from the dark rate (% level). On the other hand data at $\lambda = 800$ nm need an additional exponential term, with typical time scale of 1 ns and integral contribution at the level of few 10%. Such slow component might be related to carriers generated by long wavelengths in the neutral regions beneath the depleted layer and reaching the latter by diffusion. The characteristic time is compatible with $\tau \sim L^2/\pi D$ [6] where L is the electron diffusion length and D is the electron diffusion coefficient in silicon. In the following we'll focus on the dominant contribution to the resolution, i.e. the gaussian part, and discuss the related sigma σ_t term extracted from the fit.

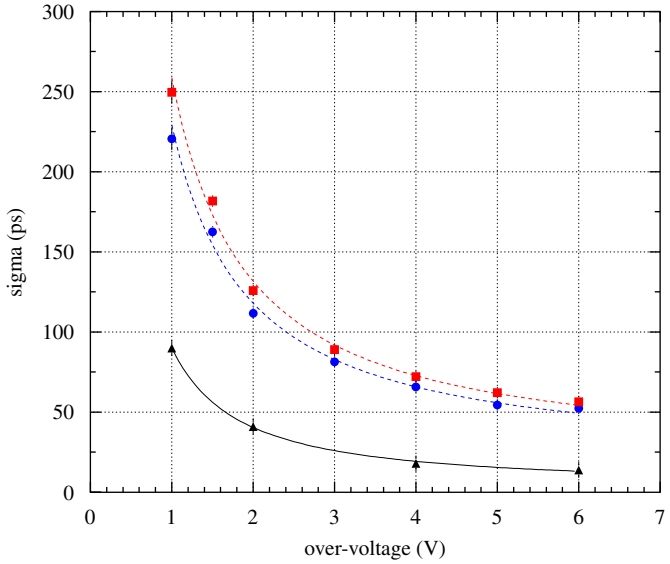

Fig. 2. Time resolution σ_t as a function of over-voltage at $\lambda = 400$ nm (circles) and at $\lambda = 800$ nm (squares). Better resolution is reached at shorter wavelengths. The electronic noise contribution is directly measured (triangles) to be small compared to the device resolution. Lines are for eye guiding.

Fig. 2 shows the resolution (σ_t) as a function of the over-voltage (ΔV) for one of the IRST devices. The resolution for the single photo-electron is at the level of 70 ps under standard working conditions ($\Delta V \sim 3-4$ V) and reaches the level of 50 ps at $\Delta V \sim 6$ V. The results for all the measured IRST devices are in fair agreement. The shape of the resolution as a function of ΔV is in qualitative agreement with the results in Ref. [7]. Statistical fluctuations in the avalanche development are due mainly to lateral propagation [8–10]. Work is in progress to simulate the timing

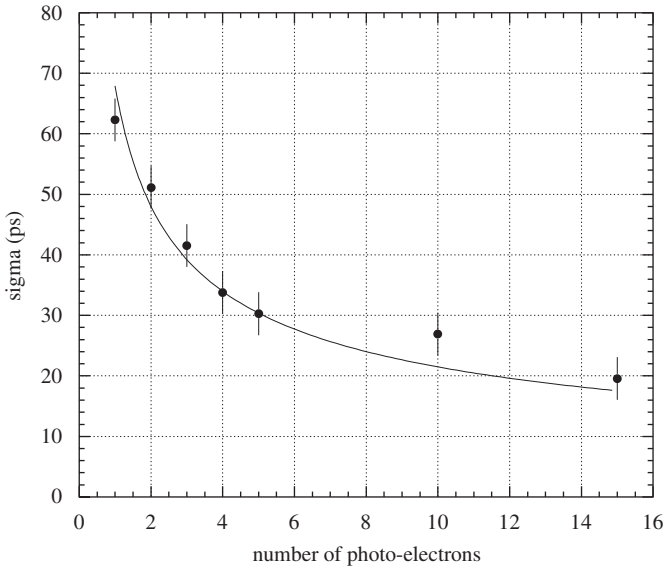

Fig. 3. Time resolution σ_t as a function of the number of simultaneous photoelectrons $N_{p.e.}$ at $\lambda = 400\,nm$ and over-voltage $\Delta V = 4\,V$ (circles). The best fit to the function $\sim 1/\sqrt{N_{p.e.}}$ (Poisson statistics) is also shown (line).

properties of the IRST devices. The worse resolution at long wavelengths (800 nm) may be explained by additional fluctuations on the longer drift time for carriers generated in depth by long wavelengths with respect to carriers generated near the high field region by short wavelengths.

The systematic uncertainties on the measurement are dominated by the contribution from the electronic noise which is directly measured as follows. Keeping the same laser and SiPM setup after every standard measurement data were collected with the electronics modified in order to evenly split the amplifier output signal, delay one component and recombine back the two components. As a result, for every s.p.e. peak from the SiPM two peaks at fixed delay were obtained at the amplifier output. The same optimum timing analysis described above is used for measuring the fixed delay and its fluctuation (solid line in Fig. 2), which includes contribution of the electronic noise to the time resolution. This contribution is small compared (in quadrature) to the measured SiPM time resolution and is not corrected for. Only the uncertainty on the noise contribution is accounted in the measured SiPM time resolution. Residual systematic uncertainties (dependence on light intensity, sampling clock jitter, etc.) are estimated at a level below 10 ps.

Timing measurements with different beam spot size (circular with diameter in the range $10-200\,\mu m$) and illuminating different cells on the SiPM surface were performed by means of pinholes and careful positioning. No relevant spread in resolution was observed, indicating uniformity in rise-time for the avalanche signal among the different cells.

Data taking under higher light intensity conditions and special trigger were performed for investigating the timing resolution in presence of >1 simultaneous photo-electrons. The dependence of σ_t as a function of the number of photo-electrons is shown in Fig. 3 to be in fair agreement with Poisson statistics. The resolution with 15 photo-electrons, typical of applications where SiPM are coupled to small volume high light yield scintillators, is better than 25 ps.

For comparison, Green-red sensitive and Blue sensitive type devices, commercially available at Photonique [11] were also studied. Their time resolution was measured with the same setup and under the conditions already described. The best resolution, obtained at the maximum over-voltage which the devices can be operated without discharges, for green-red sensitive devices is comparable, at $\lambda = 800\,nm$, to the resolution of IRST devices. At $\lambda = 400\,nm$ green-red devices perform a factor of 2 worse ($\sigma_t \sim 140\,ps$). Blue sensitive devices perform even worse: the best resolutions at $\lambda = 800\,nm$ (400 nm) are, respectively, $\sigma_t \sim 130\,ps$ (440 ps).

4. Conclusions

The technology under development at IRST for blue light optimized SiPM is well advanced with good device production yield ($>80\%$) and performance reproducibility. The measured photo-detection efficiency shows that the most critical factor involved, namely the quantum efficiency, has been successfully optimized to a very high level ($>90\%$). The avalanche triggering probability is compatible with the expectations. The fill factor will be optimized in future layouts to more than 50%.

Single photon timing resolution, in typical working conditions, is measured at the level of $<70\,ps$, with good cell-to-cell uniformity. The time resolution scales with the number of photo-electrons as expected from Poisson's statistics. Non gaussian tails in the resolution are found only for long wavelengths and not at $\lambda = 400\,nm$.

In addition to the development of SiPM, various applications are being studied by the DASIPM collaboration. Concerning medical applications, for instance, matrices of SiPM are being produced at IRST for being exploited in PET devices. Notably the energy resolution to 511 keV gammas was measured [12] at the level of $\sigma_E/E \sim 10\%$ for IRST devices ($1 \times 1\,mm^2$ cross section) coupled to an LSO crystal.

References

[1] C. Piemonte, Nucl. Instr. and Meth. A 568 (2006) 224.
[2] C. Piemonte, et al., IEEE Trans. Nucl. Sci. NS-54 (1) (2007) 236.
[3] C. Piemonte, et al., Proc. IEEE Nucl. Sci. Symp. 2006 conf. record N42-4.
[4] W. Oldham, et al., IEEE Trans. Electron Devices ED-19 (9) (1972) 1056.
[5] T.H. Wilmshurst, Signal recovery from noise in electronic instrumentation, A. Hilger Publ., 1985.
[6] S. Cova, et al., NIST Workshop on Single Photon Detectors (2003).
[7] A. Spinelli, L. Lacaita, IEEE Trans. Electron Devices ED-44 (11) (1997) 1931.
[8] P.P. Webb, R.J. McIntyre, RCA Eng. 27 (1982) 96.
[9] A. Lacaita, et al., Appl. Phys. Lett. 57 (5) (1990) 489.
[10] A. Lacaita, et al., Appl. Phys. Lett. 62 (6) (1993) 606.
[11] S.A. Photonique, Switzerland, ⟨http://www.photonique.ch⟩.
[12] To be reported in a forthcoming paper.